Stochastic modeling of some aspects of biofilm behavior

R.F. Rodríguez*
Departamento de Física Química, Instituto de Física,Universidad Nacional Autónoma de México,
Apartado Postal 20-364, 01000 México, D.F.
e-mail: zepeda@fisica.unam.mx

J.M. Zamora* and E.Salinas-Rodríguez*
Departamento de I. P. H., Universidad Autónoma Metropolitana, Iztapalapa,
Apartado Postal 55-534, 09340 México, D.F.

E. Izquierdo
Facultad de Química, CIPRO, ISPJAE,
Apartado Postal 19390, La Habana, Cuba.

Recibido el 17 de octubre de 2002; aceptado el 6 de noviembre de 2002

A unified stochastic description of the effects of internal and external fluctuations on the thickness and roughness of a biofilm is given in terms of linear and nonlinear master equations (ME). In the absence of detachment the ME is linear, while erosion renders it to be nonlinear. For the linear case the influence of the environment is modeled through an external noise in one of the transition probabilities per unit time and the ME is solved analytically. For the nonlinear case we only consider internal fluctuations and use van Kampen's systematic expansion to solve the ME. In both cases the thickness and roughness dependence on time is calculated and expressed in terms of the first two moments of the probability distribution function. An analytical expression for roughness as a function of thickness is also obtained in both cases. For both cases we compare our analytical results with reported experimental measurements of these quantities for P. *Aeruginosa.* The best fitting values of the transition probabilities and external noise parameters are determined, so that the relative error δ between the calculated and the experimentally measured values of the thickness and roughness is minimized. We find that for the linear case the mean relative error $< \delta >$ is relatively small, 1.8 %-6.2 %, while in the presence of detachment is slightly higher, 6.7 %- 9.3 %. We close the paper by discussing the advantages, scope and limitations of our approach.

Keywords: Biofilm; thickness; roughness; stochastic processes; master equation; external noise.

Se presenta una descripción unificada de los efectos producidos por fluctuaciones internas y externas sobre el espesor y la rugosidad de una biopelícula en términos ecuaciones maestras (ME) lineales y no lineales. En ausencia de desprendimiento la ME es lineal, pero la presencia de erosión la hace no lineal. En el caso lineal la influencia del ambiente se modela introduciendo ruido externo en una de las transiciones de probabilidad por unidad de tiempo y la ME se resuelve analíticamente. Para el caso no lineal sólo consideramos fluctuaciones internas y utilizamos el desarrollo sistemático de la ME introducido por van Kampen para resolverla en forma aproximada. En ambos casos la dependencia temporal del espesor y la rugosidad se calculan y expresan en función de los dos primeros momentos de la función de distribución de probabilidad. También se obtienen expresiones analíticas para la rugosidad en función del espesor y se comparan éstos resultados analíticos con mediciones experimentales reportadas para P. Aeruginosa. Se determinan los valores óptimos de las probabilidades de transición y de los parámetros de ruido externo de tal manera que el error relativo δ entre los valores calculados y medidos del espesor y la rugosidad sea mínimo. Así encontramos que para el caso lineal el error relativo medio $< \delta >$ es relativamente pequeño, 1.8%-6.2%, mientras que en presencia de desprendimiento es ligeramente mayor, 6.7%-9.3%. Concluimos discutiendo las ventajas, perspectivas y limitaciones de nuestro enfoque del problema.

Descriptores: Biopelículas, procesos estocásticos; espesor; rugosidad; ecuación maestra; ruido externo.

PACS: 05.40.-a, 05.40.Ca, 87.68.+z

1. Introduction

A biofilm is a layer-like aggregation of cells and cellular products attached to a solid surface or substratum [1, 2]. An established biofilm structure comprises microbial cells and extracellular polymeric substances, has a defined arquitecture, and provides an optimal environment for the exchange of genetic material between cells. Communication between cells may in turn affect biofilm processes such as detachment.

Biofilms occur in a large variety of engineering systems such as streambeds, water pipes, groundwater aquifers, among others [3]. They play an important role in engineering processes like biological activated carbon beds, land systems or wastewater treatment and other chemical processes, where high biomass concentrations, which allow large volumetric loading, are maintained without the need for solids separation and recycling [4]. In spite of their utility, though, biofilms can also create industrial and practical problems, such as the prevention of heat flow across a surface or the increase of the rate of corrosion at a surface [5]. This illustrates the role played by biofilms in certain infectious diseases and their importance for public health.

A clear picture of attachment can not be obtained without considering the effects of the substratum, condition-

ing films forming on the substratum, hydrodynamics of the medium, phyicochemical characteristics the medium, and various properties of the cell surface. Biofilm arquitecture is heterogeneous both in space and time, constantly changing because of external and internal processes. Although from a macroscopic point of view an idealized biofilm is a thin homogeneous layer of constant thickness, microscopically it is a nonuniform structure characterized by a variable thickness and polymer densities [6]. This heterogeneity may play an important role in hydrodynamic fouling, microbial influenced corrosion, substrate conversion [7] and biocide efficacy [8]. Also, owing to their irregular surface, biofilms increase the fluid's frictional resistance [5] and the wall shear stress [9]. These effects, in turn, influence the effective diffusion coefficient in aerobic biofilms, where the oxygen distribution strongly depends on flow conditions and on the biofilm's structure [10, 11].

In the usual macroscopic description of biofilms two variables are commonly used to characterize them, namely, thickness, E, and the aereal density S. The latter is the amount of dry biomass which is attached to a unit area of substratum and that it depends on environmental conditions. The solid surface may have several characteristics that are important in the attachment process, for instance the extent of microbial colonization appear to increase as the surface roughness increases. This is because shear forces are diminished, and surface area is higher on rougher surfaces [5]. The roughness, R, describes the standard deviation of the thickness and helps to characterize the spatial inhomogeneity within the biofilm [2]. Usually E is defined as the perpendicular distance from the substratum to the biofilm-bulk liquid interface and determines the distance through which substrates and nutrients must diffuse to fully penetrate a biofilm. In the usual macroscopic descriptions of biofilms, these state variables E and R, obey deterministic equations. However, it is observed that E may exhibit significant spatial or temporal variations even under conditions of constant substrate loading and shear stress [2, 12]. Although these variations may be accounted for in a statistical way, a deterministic approach cannot describe their dynamics or predict its values [12, 13], because strictly speaking roughness is a random, rather than a deterministic variable. Thus, the previous one-dimensional view of E should be enlarged due to the complexity of biofilm processes, and may be viewed as the outcome of intrinsic probabilistic elementary events like the birth and death of individuals in the biofilm's population, and of complex mechanisms for nutrient mass transport, such as diffusion or convection [14]. Here we shall adopt a stochastic approach and consider E as a random variable and, accordingly, the roughness, R, describes the fluctuations around the average thickness value. It depends on the number of microorganisms present, n, which is itself a stochastic variable. From this point of view, the behavior of thickness and its influence on other properties of the biofilm, should be accounted for within the framework of a stochastic description of the biofilm [15, 16]. The basic purpose in this work is to construct simple stochastic models which allow us to describe some of the complex and large variety of processes occurring in a biofilm.

Now, it is well known that fluctuations acting in open systems may be conveniently classified into internal and external fluctuations. The former are those self-originated in the system, while the latter are determined by the environment. Internal fluctuations are a consequence of the large number of microscopic degrees of freedom of a many body system, and are, therefore, averaged out in a macroscopic description. They scale with the size of the system and vanish in the thermodynamic limit, except at a critical point where long range order is established [17]. Their study is an important and well known part of statistical mechanics [18]. In contrast, external fluctuations exist when a system is under the influence of external noise, caused by a natural or induced randomness of the environment of the system. These fluctuations play the role of an external field driving the system and they do not scale with its size [19]. Thus, if external noise is present in a macroscopic system it will dominate over internal fluctuations [20].

In this work we construct a stochastic model for the behavior of the biomass fluctuations in a monospecies biofilm. We follow an approach that we used in previous work [21] and the elementary events of birth and death of individuals are assumed to be Markovian stochastic processes. Thus the stochastic time evolution of the biofilm may be described by a Markovian master equation (ME). The attachment of the biofilm is a complex process regulated by diverse characteristics of the growth medium, substratum and cell surface. Furthermore, the biofilm structure may also be influenced by the interaction of particles of nonmicrobial components from the host environment.We shall model the influence of the environment as external noise acting on one of the transition probabilities per unit time for the elementary events. The dynamics of the fluctuations is described by means of a unified treatment of internal and external fluctuations introduced by Sancho *et al.* [22]. As will be shown below, this model is capable of predicting the relationship between the average values of biofilm thickness and roughness, owing to the combined action of internal and external fluctuations.

To this end the paper is organized as follows. In the next Sec. 2 we define the model and write down the basic ME describing the time evolution of the corresponding probability density. In the absence of detachment the ME is linear, while erosion renders it to be nonlinear. This means that in the former case the transition probabilities per unit time are constant or linear functions of the number of microorganisms, n, while in the latter case they become nonlinear functions of it. In the linear case the random influence of the environment is modelled by introducing an external, non-white, dichotomic noise, into the transition probability per unit time for an organism to reproduce. Then the partial differential equation for the associated generating function (GF) is derived [15]. Since the transition probabilities also appear as parameters in this equation, this procedure generates a stochastic partial

differential equation for the GF which becomes a functional of the noise source. Averaging this equation over the realizations of the external noise source, an equation for the effective generating function (EGF) is obtained, and from it equations for the first two moments of the corresponding effective probability distribution are derived. From these quantities the relationship between roughness and average biofilm thickness is obtained as a function of time and of the parameters defining both, internal fluctuations and external noise. In the absence of external noise, in Sec. 3 the effect of detachment is considered and the corresponding nonlinear ME is constructed. We use van Kampen's systematic expansion of the ME [15] and derive a linear Fokker-Planck equation (FPE) with constant coefficients from which equations for E and R are derived and solved. In Sec. 4 we compare our analytical results for these quantities in both cases, with their experimental values, as obtained by Peyton [2] for a specific steady-state biofilm, namely, *P. Aeruginosa*. The best fitting values of the transition probabilities per unit time and external noise parameters are determined so that the relative error between the calculated and the measured values of biofilm thickness and roughness is minimized. We find that theory predicts the same type of behavior than the experiment with errors that range between $1.8\% - 6.2\%$ and $6.66\% - 9.29\%$ for the linear and nonlinear cases, respectively. Finally, we close the paper by emphasizing the scope and limitations of our approach.

2. Stochastic modeling

2.1. Internal fluctuations: constant transition probabilities

Consider a biofilm of a species of bacteria with n individuals at time t. If the processes of reproduction and death of the individuals are considered as stochastic events, n becomes a time dependent stochastic variable. Furthermore, if the age of the biofilm is ignored, the time evolution of $n(t)$ may be represented by a stochastic Markovian processes. In general, n may be space dependent, but as a first approximation to the problem this dependence will be neglected and the state of the biofilm will be specified only by $n(t)$. We assume that the number of microorganisms only changes by one, so the process is also a one step process. The time evolution of the conditional probability density,

$$P(n,t) \equiv p_n(t) \equiv P(n,t;n_0,t_0),$$

of having n microorganisms present in the biofilm at time t, given that at the initial time their number n_0 was fixed, obeys the usual master equation (ME) with the general form [15, 16],

$$\frac{\partial P(n,t)}{\partial t} = R(n+1)P(n+1,t) + G(n-1)P(n-1,t) - [R(n)+G(n)]P(n,t). \quad (1)$$

Here $R(n)$ and $G(n)$ denote, respectively, the so called recombination and generation transition probabilities per unit time that, being at n, a jump to $n-1$ or to $n+1$ occurs. These probabilities are extensive quantities, that is,

$$R(n) \equiv Vr(n), G(n) \equiv Vg(n),$$

where V is the volume of the biofilm. $r(n)$ is the natural death rate of an individual and $g(n)$ is the probability to produce a second individual by fission; both quantities are defined per unit time and unit volume. In general, both, r and g are arbitrary functions of n.

Although the differential-difference equation, (1), gives a complete description of the problem, it is easier to use the complete representation provided by the generating function (GF), $F(z,t)$, defined by

$$F(z,t) \equiv \sum_{n=0}^{\infty} \mathrm{z}^n P(n,t), \quad (2)$$

which yields $P(n,t)$ and its moments through the general relations [23]

$$P(n,t) = \frac{1}{n!}\left[\frac{\partial^n}{\partial z^n} F(z,t)\right]_{z=0}, \quad (3)$$

$$\langle n^m \rangle \equiv \sum_{n=0}^{\infty} n^m P(n,t) = \left[(z\frac{\partial}{\partial z})^m F(z,t)\right]_{z=1}. \quad (4)$$

We shall consider first the simplest case where $r(n) \equiv \alpha$ and $g(n) \equiv \beta$ are fixed constants. Then Eq. (1) reduces to

$$\dot{p}_n = \alpha V(E-1)p_n + \beta V(E^{-1}-1)p_n, \quad (5)$$

where the action of the step operators $E^{\pm}$ is defined for an arbitrary function $f(n)$ by

$$E^{\pm} f(n) = f(n \pm 1). \quad (6)$$

For this case $F(z,t)$ obeys the differential equation

$$\frac{\partial F(z,t)}{\partial t} = V[\beta(z-1) + \alpha(\frac{1}{z}-1)]F(z,t), \quad (7)$$

whose exact and analytic solution is well known [15]. In previous work we have generalized this equation into a stochastic equation by introducing external noise into one of the transition probabilities per unit time to model the dynamics of the process of imbibition in a Hele-Shaw cell [21]. Here we shall use a similar approach to describe the behavior of internal and external fluctuations in a biomembrane to derive expressions for its thickness and roughness.

2.2. Effects of external noise

To introduce external noise into (7), we assume that under a natural or induced randomness of the environment, the generation transition probability per unit time β becomes a random quantity instead of being constant [21]. That is

$$\beta = \beta_0 + \zeta(t), \quad (8)$$

where the mean value $\beta_0 \equiv \overline{\beta}$ is a positive quantity and $\zeta(t)$ denotes the fluctuations around β_0 induced externally into the system.

To describe in a unified way both, the dynamics of the internal as well as the external fluctuations of n, we use the approach developed by Sancho and San Miguel [22] and reviewed in Rodríguez *et al.* [21]. Therefore in this section we only write down explicitly some of the relevant steps. Substitution of (8) into (7) leads to the following stochastic partial differential equation for the GF in the presence of external noise

$$\frac{\partial F(z,t)}{\partial t} = V\left[\beta_0(z-1)+\alpha(\frac{1}{z}-1)+(z-1)\zeta(t)\right]F(z,t). \quad (9)$$

This defines $F(z,t)$ as a *functional* of $\zeta(t)$.

Averaging this equation over the realizations of the so far arbitrary external noise $\zeta(t)$, indicated by an overbar, an equation for the effective generating function (EGF),

$$\overline{F}(z,t) \equiv \overline{F(z,t)}, \quad (10)$$

is obtained, namely,

$$\frac{\partial \overline{F}(z,t)}{\partial t} = V\left[\beta_0(z-1)+\alpha(\frac{1}{z}-1)\right]\overline{F}(z,t)+V(z-1)F_1(z,t), \quad (11)$$

where we have identified

$$F_1(z,t) \equiv \overline{\zeta(t)F(z,t)}. \quad (12)$$

Equation (11) will become a closed equation for $\overline{F}(z,t)$ only if an independent equation for $F_1(z,t)$ is provided. Following the method described in Ref. 21, one can show that for the case under consideration this closed set of equations reads

$$\frac{\partial}{\partial t} f_i = M_{ij} f_j, \quad (13)$$

with

$$f_i = \begin{pmatrix} \overline{F}(z,t) \\ F_1(z,t) \end{pmatrix} \quad (14)$$

and

$$M_{ij} = V\begin{pmatrix} \beta_0(z-1)+\alpha(\frac{1}{z}-1) & (z-1) \\ \eta(t,t)(z-1) & -\frac{\lambda}{V}+[\beta_0(z-1)+\alpha(\frac{1}{z}-1)] \end{pmatrix}. \quad (15)$$

Here λ^{-1} denotes the correlation time of the external noise and $\eta(t,t')$ stands for its autocorrelation function.

Equation (13) can be solved exactly for appropriate initial and boundary conditions that we choose as follows. We take the initial conditions

$$\overline{F}(z,t=0) = z^{n_0}, \quad (16)$$

$$F_1(z,t=0) = 0, \quad (17)$$

which amount to assume

$$\overline{P}(n,t=0) = \delta_{n,n_0}, \quad (18)$$

where $\overline{P}(n,t)$ is the effective probability distribution associated with the EGF, $\overline{F}$. As usual, δ_{ij} denotes the Kronecker's delta. As for the boundary condition we take one that preserves the normalization of $\overline{P}(n,t)$, namely,

$$\overline{F}(z=1,t) = 1. \quad (19)$$

To solve Eq. (13) we must first specify the so far arbitrary noise parameters λ^{-1} and $\eta(t,t)$. In order to induce a mathematical model structure suitable for analytical treatment, we shall follow Sancho and San Miguel [22] and make the assumption that $\zeta(t)$ is a two-state or dichotomic Markov process. This means that the stochastic variable n is a stepwise constant process which jumps between two discrete values $\pm\Delta$ with equal probability at instants randomly distributed and with a correlation time λ^{-1}. More explicitly, this implies that $\zeta(t)$ is defined by the properties

$$\overline{\zeta(t)} = 0 \quad (20)$$

and

$$\overline{\zeta(t)\zeta(t')} = \Delta^2 e^{-\lambda|t-t'|}, \quad (21)$$

so that

$$\eta(t,t) \equiv \overline{\zeta(t)\zeta(t)} = \Delta^2. \quad (22)$$

We may view this dichotomic noise as a representation of a random feature of the natural environment of the biofilm which either favors or opposes the birth of individuals. It models a situation where two states of the environment have the same intensity but opposite effect on the system, without specifying more details of how this influence is produced. It should be mentioned that a dichotomic noise is not as unrealistic as could be presumed. Actually, it may be easily produced in the laboratory with a noise generator and can be actually applied to real systems [20]. On the one hand, this noise has the advantage of being itself simple enough for easy, explicit mathematical manipulation, and will be used as a first exploratory representation of the effects of external noise on the biofilm. Furthermore, the positive character of β_0 and V imposes the condition $[\beta_0 - \Delta] \geq 0$ on the values of Δ, and this in turn guarantees the positivity of $P(n,t)$, otherwise the starting equation (9) would be meaningless. This positivity might be violated for white noise [15].

The solution of Eq. (13) with (16)- (17) yields for $\overline{F}(z,t)$ and $F_1(z,t)$

$$\overline{F}(z,t) = \frac{z^{n_0}}{2\Lambda(z)} e^{\left[a(z)-\frac{\lambda-\Lambda(z)}{2}\right]t} \times \left[(\lambda+\Lambda(z)) + (\lambda-\Lambda(z))\, e^{-\Lambda(z)t}\right], \quad (23)$$

$$F_1(z,t) = \frac{\lambda^2 - \Lambda^2(z)}{4b(z)\Lambda(z)} e^{[a(z) - \frac{\lambda - \Lambda(z)}{2}]t}(1 - e^{-\Lambda(z)t}), \quad (24)$$

where the following abbreviations have been used,

$$\Lambda(z) \equiv \left[\lambda^2 + 4\Delta^2 b^2(z)\right]^{1/2}, \quad (25)$$

$$a(z) \equiv V\left[\beta_0(z-1) + \alpha(\frac{1}{z} - 1)\right], \quad (26)$$

$$b(z) \equiv V(z-1). \quad (27)$$

From Eqs. (23) and (4) we get the first two moments of the effective distribution probability $\overline{P}(n,t)$ associated with $\overline{F}(z,t)$,

$$\langle \overline{n}(t) \rangle = n_0 + V(\beta_0 - \alpha)t \quad (28)$$

and

$$\langle \overline{n^2}(t) \rangle = n_0[2V(\beta_0 - \alpha)t - 1 + n_0] + 2\Gamma V^2(1 + e^{-\lambda t}) + 2\alpha V t + V^2(\beta_0 - \alpha)^2 t^2, \quad (29)$$

where $\Gamma \equiv \Delta^2/\lambda^2$. As a consequence, the standard deviation σ_n^2 and the relative fluctuation χ_n turn out to be, respectively,

$$\sigma_n^2 \equiv \left\langle \overline{n^2} \right\rangle - \langle \overline{n} \rangle^2 = 2\Gamma V^2(1 + e^{-\lambda t}) + 2\alpha V t - n_0 \quad (30)$$

and

$$\chi_n \equiv \frac{\sigma_n^2}{\langle \overline{n} \rangle^2} = \frac{1}{V(\beta_0 - \alpha)^2(N_0 + t)^2}[N_0(\beta_0 - \alpha) + 2\alpha t + 2\Gamma V(1 + e^{-\lambda t})], \quad (31)$$

with

$$N_0 \equiv \frac{n_0}{V(\beta_0 - \alpha)}.$$

It is convenient to rewrite this last equation in the static limit of the external noise, $\lambda^{-1} \to \infty$, and in the thermodynamic limit defined by $n \to \infty, V \to \infty, n/V =$ finite, which leads to

$$\chi_n = \frac{\Delta^2 t^2}{[\frac{n_0}{V} + (\beta_0 - \alpha)t]^2}. \quad (32)$$

Equations (28) and (32) show that the mean value $\langle \overline{n}(t) \rangle$ is independent of the external noise, whereas χ_n have terms that depend on both, internal and external fluctuations as well. The latter contributions depend on the amplitude Δ of the dichotomic noise and remain finite in the thermodynamic limit, but the contribution due to internal fluctuations vanishes in this limit.

3. Effects of detachment

Biofilm cells may be dispersed either by shedding of doughter cell from actively growing cells, detachment as a result of nutrient levels or quorum sensing, or shearing of biofilm aggregates because of flow effects. The mechanisms underlying these processes are not well understood. Detachment caused by physical forces has been studied in detail, and the main processes causing it are erosion or shearing (continuous removal of small portions of the biofilm), sloughing (rapid and massive removal), and abrasion (detachment due to collision of particle from the bulk fluid with biofilm) [24, 25].

As a first approach to the description of these complex processes, here we model detachment in terms of the following simple stochastic point of view. We assume that the growth of the biofilm is modeled with linear generation and natural death rates, that is, $g(n) = \beta n$ and $r(n) = \alpha n$. If detachment of biomass may exist, for each individual there will be an additional death rate, $r_d(n)$, which can be estimated as follows. Experimental results [6] provide a basis to assume that for each microorganism, the detachment frequency varies with the depth in the biofilm and is inversely proportional to the area of substratum A_b. Then, if the volume of all the microorganisms and their metabolic products is $V_m = v_m n$, the additional detachment probability per unit time should also be proportional to the number of the other individuals present [26],

$$r_d(n) = \frac{\gamma}{\Omega_0} n(n-1), \quad (33)$$

with $\gamma \equiv k_d V^{1/3}$, where k_d is the detachment rate. We have also introduced the dimensionless quantity

$$\Omega_0 \equiv \Omega V^{1/3}, \quad \text{with} \quad \Omega \equiv \frac{A_b(1 - \epsilon_b)}{v_m},$$

being ϵ_b the mass porosity of the biofilm, *i. e.,* the volume fraction of water in the total biomass volume V. Thus, the total recombination probability is now nonlinear,

$$r(n) \simeq \alpha n + \frac{\gamma}{\Omega_0} n(n-1) \quad (34)$$

and the macroscopic rate equation reads

$$\frac{1}{V}\frac{dn}{dt} \equiv \dot{n} = g(n) - r(n) = (\beta - \alpha)n - \frac{\gamma}{\Omega_0} n(n-1). \quad (35)$$

The corresponding nonlinear ME for $p_n(t)$ per unit volume is the following differential-difference equation

$$\dot{p_n} = \left[\alpha(n+1) + \frac{\gamma}{\Omega_0} n(n+1)\right] p_{n+1} + \beta(n-1)p_{n-1} - \left[\alpha n + \frac{\gamma}{\Omega_0} n(n-1) + \beta n\right] p_n, \quad (36)$$

which using (6) may be rewritten in the more compact form

$$\dot{p_n} = \alpha(E-1)np_n + \beta(E^{-1} - 1)np_n + \frac{\gamma}{\Omega_0}(E-1)n(n-1)p_n. \quad (37)$$

3.1. The systematic expansion

The ME (36) is nonlinear in the sense that $r(n)$ is a nonlinear function of n. This equation cannot be solved analytically in an exact form and it is necessary to develop an approximate analytical solution. To this end we use van Kampen's general method and expand (36) in powers of Ω^{-1} [15]. To this end first note that the transition probabilities $r(n)$ and $g(n)$ are independent of Ω and that we have to postulate the way in which $p_n(t)$ depends on Ω. Following van Kampen, we assume that $p_n(t)$ has a sharp peak located at some value n of order Ω and located at the point $\Omega\phi(t)$, with a width of order $\Omega^{1/2}$. This assumption is expressed formally by transforming the stochastic variable n to a new variable ζ defined by

$$n = \Omega_0\phi(t) + \Omega_0^{1/2}\zeta, \tag{38}$$

where $\phi(t)$ is some time dependent function that has to be determined. This assumption contains a central-limit theorem argument and its correctness has to be justified *a posteriori* by showing that it is actually possible to choose $\phi(t)$ in such a way that ζ turns out to be of order unity, by adjusting $\phi(t)$ to follow the motion of the peak. As a consequence, $p_n(t)$ transforms into a probability density distribution $\Pi(\zeta,t)$ according to the relation

$$p_n(t) = p(n,t) = p\left[\Omega_0\phi(t) + \Omega_0^{1/2}\zeta, t\right] \equiv \Pi(\zeta,t). \tag{39}$$

Since the probability should be conserved in terms either of n or ζ, it then follows that

$$p(n,t) = \Omega_0^{-1/2}\Pi(\zeta,t) \tag{40}$$

and that the derivatives transform as

$$\frac{\partial p}{\partial n} = \Omega_0^{-1}\frac{\partial \Pi}{\partial \zeta} \tag{41}$$

and

$$\frac{\partial p}{\partial t} = \Omega_0^{-1/2}\frac{\partial \Pi}{\partial t} - \frac{d\phi}{dt}\frac{\partial \Pi}{\partial \zeta}. \tag{42}$$

Starting from (36), it is a matter of straightforward algebra to obtain the following transformed equation for $\Pi(\zeta,t)$

$$\frac{\partial \Pi}{\partial t} - \Omega_0^{1/2}\frac{d\phi}{dt}\frac{\partial \Pi}{\partial \zeta} = \Omega_0^{1/2}\{[\alpha\phi(t) - \beta\phi(t) + \gamma\phi^2(t)]\frac{\partial \Pi}{\partial \zeta}\} + \Omega_0^0\{[\alpha - \beta + 2\gamma\phi(t)]\frac{\partial}{\partial \zeta}(\zeta\Pi) + \frac{1}{2}[\alpha\phi(t) + \beta\phi(t) + \gamma\phi^2(t)]\frac{\partial^2 \Pi}{\partial \zeta^2}\} + \Omega_0^{-1/2}[\frac{\alpha+\beta}{2}\frac{\partial^2}{\partial \zeta^2}(\zeta\Pi) + \gamma\frac{\partial}{\partial \zeta}(\zeta^2\Pi)] + \Omega_0^{-1}[\frac{\gamma}{2}\frac{\partial^2}{\partial \zeta^2}(\zeta^2\Pi)] + \vartheta(\Omega_0^{-3/2}). \tag{43}$$

This expansion leads to the following results. The leading terms are of order $\Omega_0^{1/2}$ and they can be made to cancel by demanding that $\phi(t)$ should obey

$$\frac{d\phi}{dt} = V(\beta - \alpha)\phi - V\gamma\phi^2, \tag{44}$$

which gives the macroscopic equation (35). Note that this equation has the time independent solution

$$\phi^s = (\beta - \alpha)/\gamma \tag{45}$$

corresponding to a stationary population

$$n^s = \Omega_0\frac{\beta - \alpha}{\gamma}, \tag{46}$$

as follows from (35). To the next order Ω_0^0, (43) reduces to a linear Fokker -Planck per unit volume equation with time dependent coefficients, namely,

$$\frac{\partial \Pi}{\partial t} = [2\gamma\phi(t) - (\beta - \alpha)]\frac{\partial(\zeta\Pi)}{\partial \zeta} + \frac{1}{2}\left[(\beta + \alpha)\phi(t) + \gamma\phi^2(t)\right]\frac{\partial^2 \Pi}{\partial \zeta^2}. \tag{47}$$

For the stationary state ϕ^s, this equation reduces to the linear Fokker -Planck equation with constant coefficients

$$\frac{\partial \Pi}{\partial t} = (\beta - \alpha)\frac{\partial(\zeta\Pi)}{\partial \zeta} + \frac{\beta(\beta - \alpha)}{\gamma}\frac{\partial^2 \Pi}{\partial \zeta^2}. \tag{48}$$

Its solution is well known for the initial condition

$$\Pi(\zeta,0) \equiv \delta(\zeta - \zeta_0),$$

namely,

$$\Pi(\zeta,t) = \frac{1}{\sqrt{\frac{\beta\pi}{\gamma}[1 - e^{-2(\beta-\alpha)t}]}}\exp\left\{-\frac{\gamma}{\beta}\frac{\left[\zeta - \zeta_0 e^{-(\beta-\alpha)t}\right]^2}{1 - e^{-2(\beta-\alpha)t}}\right\}, \tag{49}$$

and becomes a stationary Gaussian around ϕ^s for $t \to \infty$,

$$\Pi^s(\zeta) = \sqrt{\frac{\gamma}{\beta\pi}}e^{-\frac{\gamma}{\beta}\zeta^2}. \tag{50}$$

3.2. The Gaussian approximation

In the limit $t \to \infty$ it suffices to determine only the first and second moments of $\Pi(\zeta,t)$. Although these quantities can be obtained directly from Eqs. (49) or (50), it is convenient, for future reference, to derive the equations they satisfy from (47). This leads to

$$\frac{\partial}{\partial t}\langle\zeta\rangle = V\left[(\beta - \alpha) - 2\gamma\phi(t)\right]\langle\zeta\rangle \tag{51}$$

and

$$\frac{\partial}{\partial t}\left\langle \zeta^2 \right\rangle = 2V\left[\beta-\alpha-2\gamma\phi(t)\right]\left\langle \zeta^2 \right\rangle + V\left[(\beta+\alpha)\phi(t)+\gamma\phi^2(t)\right]. \quad (52)$$

These equations describe the time behavior of $\langle\zeta\rangle$ and $\langle\zeta^2\rangle$ around any macroscopic state defined by $\phi(t)$. For the particular macroscopic state defined as the stationary solution (45), Eqs. (51), (52) reduce to

$$\frac{\partial}{\partial t}\left\langle \zeta \right\rangle^s = -V(\beta-\alpha)\left\langle \zeta \right\rangle^s \quad (53)$$

and

$$\frac{\partial}{\partial t}\left\langle \zeta^2 \right\rangle^s = -2V(\beta-\alpha)\left\langle \zeta^2 \right\rangle^s + 2V\frac{\beta(\beta-\alpha)}{\gamma}, \quad (54)$$

where the upperscript s denotes the stationary case. The exact solutions of these equations for given

$$\langle\zeta(t=0)\rangle^s \equiv \zeta_0, \quad \left\langle \zeta^2(t=0)\right\rangle^s \equiv \zeta_0^2,$$

read

$$\langle\zeta(t)\rangle^s = \zeta_0 \exp\left[-V(\beta-\alpha)t\right] \quad (55)$$

and

$$\left\langle \zeta^2(t)\right\rangle^s = \zeta_0^2 \exp\left[-2V(\beta-\alpha)t\right] + \frac{\beta}{\gamma}\{1-\exp\left[-2V(\beta-\alpha)t\right]\}. \quad (56)$$

From Eqs. (55) and (56) it follows that the standard deviation

$$\sigma_\zeta^2(t) \equiv \left\langle \zeta^2(t)\right\rangle^s - [\langle\zeta(t)\rangle^s]^2$$

is given by

$$\sigma_\zeta^2(t) = \frac{\beta}{\gamma}\{1-\exp\left[-2V(\beta-\alpha)t\right]\}, \quad (57)$$

and the relative fluctuation,

$$\chi_\zeta(t) \equiv \frac{\left\langle \zeta^2(t)\right\rangle^s - [\langle\zeta(t)\rangle^s]^2}{[\langle\zeta(t)\rangle^s]^2},$$

turns out to be

$$\chi_\zeta(t) = \frac{2\beta}{\gamma\zeta_0^2}e^{V(\beta-\alpha)t}\sinh[V(\beta-\alpha)t]. \quad (58)$$

In terms of the number, n, of individuals present at time t, from Eqs. (38), (55), (56) and (57), it follows that

$$\langle n(t)\rangle^s = n_0\exp\left[-V(\beta-\alpha)t\right] + \Omega_0\frac{\beta-\alpha}{\gamma}\left\{1-\exp\left[-V(\beta-\alpha)t\right]\right\}, \quad (59)$$

$$\sigma_\zeta^2(t) = \sigma_n^2(t) \quad (60)$$

and

$$\chi_n(t) = 2\beta\gamma \times \frac{e^{V(\beta-\alpha)t}\sinh[V(\beta-\alpha)t]}{[\gamma n_0 - \Omega_0(\beta-\alpha)\left\{1+\exp\left[V(\beta-\alpha)t\right]\right\}]^2}. \quad (61)$$

4. Results

In heterogeneous biofilms convection and not only diffusion, may be a significant mechanism for nutrient mass transport, a possibility that shows the complexity of biofilm processes. However, since at present it is not yet possible to describe or numerically simulate this complexity, average values of biofilm thickness must still be used for modelling and design purposes [2], [27]. Given this complexity and in order to relate the predictions of our model with experimental results, we recall that we have assumed that the biofilm is spatially homogeneous. Moreover, if v_m is the volume of an individual microorganism and its extracellular products, the volume V_m of all the microorganisms and their metabolic products is $V_m = v_m n$, where n is the number of individuals present at time t. Since the porosity ϵ_b of the biofilm is the volume fraction of water in the total biomass volume V,

$$V = \frac{v_m}{1-\epsilon_b}n. \quad (62)$$

Now, since the thickness E may be also defined as V divided by the area, A_b, of the solid surface to which the biofilm is attached, the total thickness E of the biofilm can be expressed as

$$E(t) = \frac{v_m}{A_b(1-\epsilon_b)}\,n(t) \equiv \frac{1}{\Omega}\,n(t). \quad (63)$$

Apart from E, another commonly used quantity to characterize the accumulation of a biofilm, is its coefficient of surface roughness or thickness variability, R. It describes the standard deviation of E,

$$R \equiv \sqrt{\sigma_E^2} = \frac{1}{\Omega}\sqrt{\sigma_n^2}. \quad (64)$$

4.1. Linear case

Using (28) and (63) we derive the following explicit expression for $\left\langle \overline{E}(t)\right\rangle$ as a function of t for the linear case,

$$\left\langle \overline{E}(t)\right\rangle_L = \frac{1}{\Omega}\left[n_0 + V(\beta_0-\alpha)t\right]. \quad (65)$$

Note that it does not depend on the noise parameter Δ; so, according to our model the average thickness is not sensitive to the external noise in the linear case.

It is convenient to relate Eq. (65) with experimentally measurable quantities. To this end recall that the areal density, S, is the amount of dry biomass which is attached to a unit area of substratum and that it depends on environmental conditions. Since the dimensions of the substrate loading rate, $\mathfrak{L}$, are mass/(area-time), S and $\mathfrak{L}$ are related by $\mathfrak{L} = S/t$. On the other hand, volumetric density, ρ_V, is the amount of biomass in a given volume of biofilm and it is reported as dry biomass per unit wet volume. This quantity is

important in the mathematical modeling of biofilm processes since biomass concentration is often related to the activity of a biofilm.

Similarly, from (30) in the static limit and (64) we arrive at

$$R_L(t) = \frac{1}{\Omega}\sqrt{V^2\Delta^2 t^2 + 2V\alpha t - n_0}, \qquad (66)$$

which depends explicitly on the external noise through Δ. Using Eq. (65) we get $R_L(t)$ in terms of $\left\langle \overline{E}(t)\right\rangle_L$

$$R_L\left[\left\langle \overline{E}(t)\right\rangle_L\right] = \frac{1}{\Omega(\beta_0-\alpha)}\{\Delta^2\Omega^2\left\langle \overline{E}(t)\right\rangle_L^2 + 2\Omega\left[\alpha(\beta_0-\alpha) - \Delta^2 n_0\right]\left\langle \overline{E}(t)\right\rangle_L + n_0\left(\Delta^2 n_0 - \beta_0^2 + \alpha^2\right)\}^{1/2}. \qquad (67)$$

In contrast to $\left\langle \overline{E}(t)\right\rangle_L$, $R_L(t)$ depends on the external noise through Δ. However, in the absence of external noise, $\Delta = 0$, this equation shows that roughness increases with the average thickness. Note that from Eq. (67) it also follows that roughness $R(t)$ increases when the observation area, $A_b \sim \Omega$, of the biofilm decreases. This feature is also consistent with experimental observations which show that thickness data measured by optical methods at different locations, where the observed area is very small, provide information of roughness that can not be obtained by volumetric displacement methods [2]. We also know that the increased surface roughness increases the mass transport rate to the biofilm [28].

4.2. Nonlinear case

Analogously, for the nonlinear case of Section 3, equivalent expressions to (65)-(67) are obtained from (59) and (60). This leads to

$$\left\langle \overline{E}(t)\right\rangle_{NL} = \frac{\Omega_0}{\Omega}\frac{\beta-\alpha}{\gamma}\left\{1-\exp\left[-V(\beta-\alpha)t\right]\right\} + \frac{n_0}{\Omega}\exp\left[-V(\beta-\alpha)t\right], \qquad (68)$$

$$R_{NL}(t) = \frac{1}{\Omega}\sqrt{\frac{\beta}{\gamma}\left\{1-\exp\left[-2V(\beta-\alpha)t\right]\right\}}, \qquad (69)$$

or in terms of $\left\langle \overline{E}(t)\right\rangle_{NL}$

$$R_{NL}\left[\left\langle \overline{E}(t)\right\rangle_{NL}\right] = \frac{1}{\Omega}\sqrt{\frac{\beta}{\gamma}}\frac{1}{\Omega_0\frac{\beta-\alpha}{\gamma} - n_0} \times\{n_0[n_0 - 2\Omega_0\frac{\beta-\alpha}{\gamma}] + 2\Omega\Omega_0\frac{\beta-\alpha}{\gamma}\left\langle \overline{E}(t)\right\rangle_{NL} - \Omega^2\left\langle \overline{E}(t)\right\rangle_{NL}^2\}^{1/2}. \qquad (70)$$

5. Comparison with experiment

The thickness variability of a pure culture of *P. Aeruginosa*, as a function of time and for different values of the substrate loading rate $\mathfrak{L}$, was measured by Peyton [2]. In these experiments photomicrographic images of the biofilm's cross section were captured and stored. The biofilm thickness was measured every $2x10^{-6}m$. Since the width of the sample was $5x10^{-6}m$, it may be reasonably assumed that $A_b = 10^{-11}m^2$. In the experiments it was estimated that $v_m = 2.09x10^{-18}m^3$ and $\epsilon_b = 0.9$. According to Eq. (63) this yields $\Omega^{-1} = 2.09x10^{-6}m$.

It should be recalled that in Peyton's experiments the reactor was cleaned up before each experiment and filled with nutrients, so that at the initial time there were no reproducing microorganisms in the system. Thus, for the purpose of comparing our theoretical predictions for $\left\langle \overline{E}(t)\right\rangle$ in the linear and nonlinear cases, with the corresponding measured values, we should set $n_0 = 0$ in Eq. (65).

A first comparison with experimental results is obtained if $\left\langle \overline{E}(t)\right\rangle_L$ vs. t is plotted from Eq.(65) optimizing $\Psi \equiv V(\beta_0 - \alpha)$, so that in the time interval $0 - 166.5\ hr$, the sum of squared deviations between experimental and theoretical values is minimized. The optimal values are given in Table I. In this way we get the theoretical straight lines shown in Fig. 1.

By carrying out a linear regression for each straight line, we find the best fitting values for the slope, m_{op}, with the corresponding correlation coefficient C^2. The values of m_{op} and C^2 are also given in Table I. Since $C^2 \approx 1$, the adjustment is excellent. The relative per cent error, δ, between experimental points and theoretical values is defined as

$$\delta \equiv \frac{\left\langle \overline{E}(t)\right\rangle_{\exp} - \left\langle \overline{E}(t)\right\rangle_{theo}}{\left\langle \overline{E}(t)\right\rangle_{\exp}} x100.$$

As a result, the mean relative error $\langle\delta\rangle$ of the absolute value of δ, for each straight line in Fig. 1 is also given in Table I. It ranges from 1.8% to 6.2%, and these values represent a good fitting between the linear theory and the experimental results in the initial stage, from 0 to 166.5 hr, of the development of the growing process.

Let us now consider the behavior of roughness. Equation (67) gives a nonlinear dependence of $R_L(t)$ on $\left\langle \overline{E}(t)\right\rangle_L$. Note that this theoretical relation is more general that the linear one reported in the experimental measurements by Peyton (1996) in his Fig. 3. To identify the conditions under which our result for $R_L(t)$ reduces to that of Peyton's, we recall that in the static limit of the external noise, $\lambda^{-1} \to \infty$, and in the thermodynamic limit defined by $n \to \infty, V \to \infty$, $n/V =$ finite, the relative fluctuation χ_n is given by Eq. (32). If in this equation we set $n_0 = 0$ we get

$$\chi_P^{st} = \frac{(V\Delta)^2}{\Psi^2}, \qquad (71)$$

or in terms of $R_L(t)$ and $\left\langle \overline{E}(t)\right\rangle_L$this relation reduces to the linear behavior

$$R_L\left[\left\langle \overline{E}(t)\right\rangle_L\right] = \frac{V\Delta}{\Psi}\left\langle \overline{E}(t)\right\rangle_L. \qquad (72)$$

TABLE I.

$\mathfrak{L}(mgm^{-1}h^{-1})$	$\Psi(h^{-1})$	$m_{op}x10^{-8}(mh^{-1})$	C^2	$<\delta>(\%)$
10.2	0.01771	3.701	0.9985	1.8
51.2	0.04299	8.985	0.9560	6.2
92.2	0.13517	28.25	0.9652	5.7

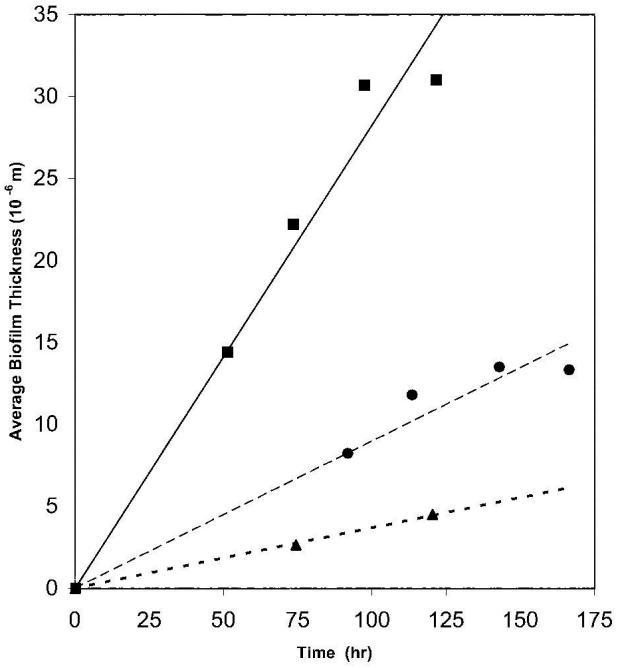

FIGURE 1. Time progression of the thickness average $\overline{E}(t)\ _L$ for *P. Aeruginosa*, as calculated from Eq. (37) for the parameters values $\Omega^{-1} = 2.09$ x 10^{-6} m, $v_m = 2.09$ x 10^{-18} m^3 , $\epsilon_b = 0.9$. The different curves correspond to the three substrate loading rates reported by Peyton, 1996 given in Table I, (▲,- - -) $\mathfrak{L}_{01} = 10.2$, (●,— —) $\mathfrak{L}_{02} = 51.2$, (,—) $\mathfrak{L}_{03} = 92.2$ $(mgm^{-1}h^{-1})$.

When the above limits are not considered, the term $\sim \left\langle \overline{E}(t) \right\rangle_L^{1/2}$ in (67) can not be neglected. To estimate a value for the resulting $\chi(t)$ we use the stationary value of $\left\langle \overline{E}(t) \right\rangle_L$, $\left\langle \overline{E} \right\rangle_L^{st}$, which corresponds to the plateau value of the average biofilm thickness in Fig. 1 in Peyton [2] and are given in our Table II,

$$\chi^{st} = \frac{(V\Delta)^2}{\Psi^2} + \frac{2}{\Omega}\frac{V\alpha}{\Psi}\frac{1}{\left\langle \overline{E} \right\rangle_L^{st}}, \tag{73}$$

or

$$R_L\left[\left\langle \overline{E} \right\rangle_L^{st}\right] = \left\langle \overline{E} \right\rangle_L^{st}\left[(\frac{V\Delta}{\Psi})^2 + \frac{2}{\Omega}\frac{V\alpha}{\Psi}\frac{1}{\left\langle \overline{E} \right\rangle_L^{st}}\right]^{1/2}. \tag{74}$$

In the last two equations the parameter $V\Delta$, which measures the influence of the external noise is not known. The value of the parameter $\Psi \equiv V(\beta_0 - \alpha)$ was optimized previously in the linear case and its values are given in Table I. To determine the best fitting value of $V\Delta$ we proceed as follows. First, for both Eqs. (72) and (74) we determine the value of $V\Delta$ and the curve that passing through the origin, represents best all the experimental points of biofilm roughness as a function of average biofilm thickness reported in Peyton's Fig. 3 [2]. These optimal values are given in Table II for Eq. (72) and $V\Delta = 0.042$ for Eq. (74). For both cases this behavior is shown in our Fig. 2, where the continuous line is the nonlinear model prediction and the broken line represents the adjustment of the experimental data given in Peyton's Fig. 3. A linear regression analysis of the experimental points yields a correlation coefficient $C^2 = 0.58$. On the other hand, carrying out the same analysis for the first term on the right hand side of Eq. (72), yields $C^2 = 0.44$. This shows that due to the dispersion of the experimental points, the model exhibits an adjustment as poor as the one in Figure 3 of Peyton [2]. This fact is a direct consequence of the absence of specific experimental data for each loading rate. However, it should be pointed out that the theoretical model consistently implies that $R_L(t)$ vanishes for zero $\left\langle \overline{E}(t) \right\rangle_L$,whereas for Peyton's regression line this is not the case.

From the above results we can now derive the condition for which the second term on the right hand side of (74) may be neglected with respect to the first. This occurs when

$$\frac{\Omega}{2\Psi}(V\Delta)^2 \left\langle \overline{E}(t) \right\rangle^{st} \gg V\alpha. \tag{75}$$

The order of magnitude of the maximum values of $V\alpha$ for which this condition holds, is given in Table II. From these values and those of Ψ given in the same Table II, we determine the corresponding value of β_0 (Table II).

When condition (75) is not fulfilled, $V\alpha$ takes a value different from the one given in Table II. We shall take the value $V\alpha = 0.4385$ in Fig. 2, which is one order of magnitud larger than those given in Table II but still consistent with Ψ.

TABLE II.

$\mathfrak{L}(mgm^{-1}h^{-1})$	$\overline{E}(t)\ ^{st} \times 10^{-6}(m)$	$\Psi(h^{-1})$	$\Delta V(h^{-1})$	$\alpha V(h^{-1})$	$\beta_0 V(h^{-1})$
10.2	4.52	0.0177	0.074	$\sim 10^{-2}$	0.0277
51.2	13.33	0.0430	0.116	$\sim 10^{-1}$	0.1430
92.2	31.00	0.1352	0.205	$\sim 10^{-1}$	0.2352

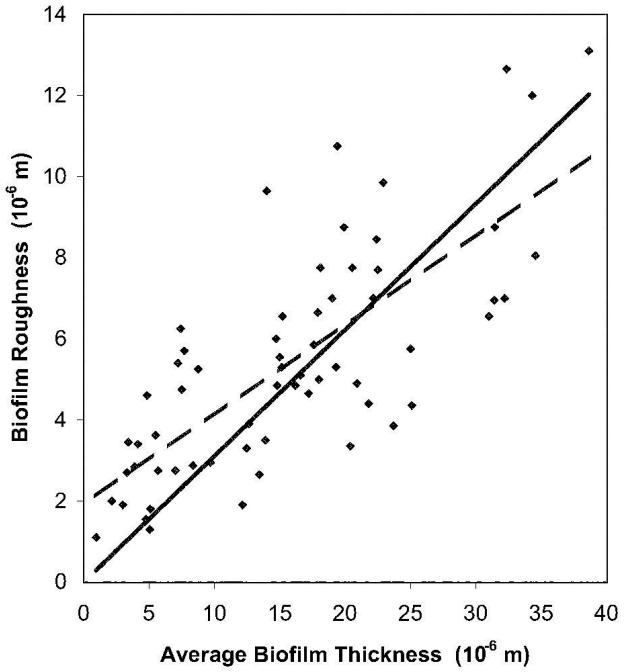

FIGURE 2. Experimental (- - -) and theoretical (—) biofilm roughness R_L vs. average biofilm thickness $\overline{E}(t)$ for the parameters given in Table II. The points are data from all the experiments reported by Peyton [2].

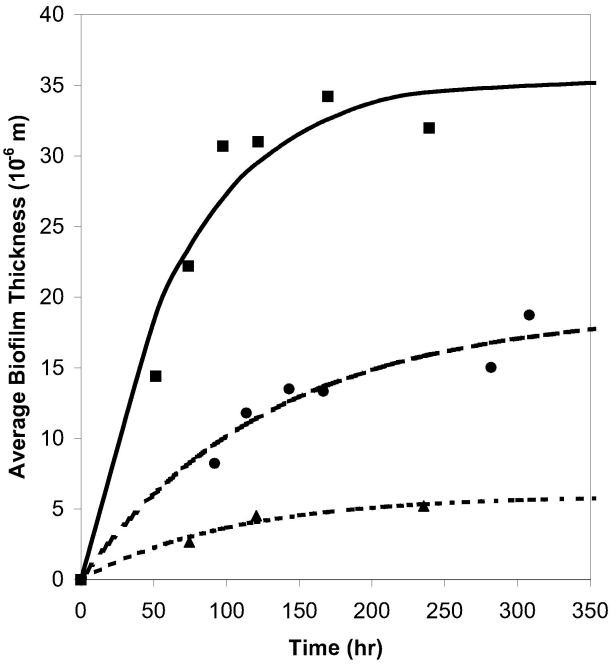

FIGURE 3. Experimental points and theoretical time progression curves of the thickness average $\overline{E}(t)_{NL}$ for *P. Aeruginosa,* the same parameters as in Fig. 1. The different curves correspond to the three substrate loading rates reported by Peyton, 1996: (- - -) $\mathfrak{L}_{01} = 10.2$, (— —) $\mathfrak{L}_{02} = 51.2$, (—) $\mathfrak{L}_{03} = 92.2$ $(mgm^{-1}h^{-1})$.

Let us now turn our attention to the nonlinear case. Note that (68) and Fig. 2, imply that the nonlinear model may describe all the behavior of the experimental curves. Indeed, if using Eq. (68) we plot $\langle \overline{E}(t) \rangle_{NL}$ vs. t and optimize the values $\Psi_{NL} \equiv V(\beta - \alpha)$ and the nonlinear parameter, $V\gamma$, for the time interval $0 - 350\ hr$, we get the curves plotted in our Fig. 3. They show that $\langle \overline{E}(t) \rangle_{NL}$ saturates after a definite time interval for the different loading rates. The relative error between experimental points and the theoretical values, $\langle \delta \rangle$, is calculated in the same way as for the linear case. The corresponding optimized values are given in Table III.

Notice that Eq. (69) predicts $R_{NL}(t)$ as a function of t and γ, separately. Since in the previous analysis we have only determined the optimal values of Ψ_{NL} for the different loading rates, it is necessary to determine first β in an independent way. To this end, note that from Eq. (69) it follows that as $t \to \infty$

$$R_A \equiv R(t \to \infty) = \frac{1}{\Omega}\sqrt{\frac{\beta}{\alpha}}. \tag{76}$$

TABLE III.

$\mathfrak{L}(mgm^{-1}h^{-1})$	$\Psi_{NL}(h^{-1})$	$V\gamma x10^{-2}(h^{-1})$	$< \delta > (\%)$
$(\mathfrak{L}_1)10.2$	0.0095	0.1596	6.66
$(\mathfrak{L}_2)51.2$	0.0077	0.0404	6.73
$(\mathfrak{L}_3)92.2$	0.0145	0.0408	9.29

Although no explicit experimental results for this limit R are available, we can get an estimated limit value for each of the experimental loading rates as follows. From Eq. (68) we get the asymptotic values $\langle \overline{E}(t \to \infty) \rangle_{NL} \equiv \langle \overline{E}(t) \rangle_{NL}^{A}$, reported in Table IV. Next, from Peyton's Fig. 3, we get estimated limit values for R_A, by averaging the two experimental data nearest to the determined values for $\langle \overline{E}(t) \rangle_{NL}^{A}$. Finally, from Eq. (76), we obtained the values of the parameter β/γ for each loading rate. For the same values of Ψ given in Table IV, and the corresponding values of β/γ, Eq.(69) is used to generate the analytical curves plotted in Fig. 4.

From Figs. 3 and 4, we may identify two stages of the biofilm growing process. The first one is characterized by a high growing rate of both, $\langle \overline{E}(t) \rangle_{NL}$ and $R_{NL}(t)$. Roughly, the high growing rate stage can be identified in both figures as $0 < t < 50$, $0 < t < 100$, and $0 < t < 150$ for $\mathfrak{L}_1$, $\mathfrak{L}_2$, and $\mathfrak{L}_3$, respectively. The second stage corresponds to a decreasing growing rate process leading to an asymptotic value for $\langle \overline{E}(t) \rangle_{NL}$ and R.

Equation (70) gives $R_{NL}\left[\langle \overline{E}(t) \rangle_{NL}\right]$ as a function of $\langle \overline{E}(t) \rangle_{NL}$, β/γ and $\Psi/(V\gamma)$. This relation is represented by the continuous curve in Fig. 5. As before, the broken curve is Peyton's result. Finally, we compare the experimental and theoretical curves for R vs. $\langle \overline{E}(t) \rangle$. The theoretical curve was obtained by minimizing the error between the experi-

TABLE IV.

$\mathfrak{L}(mgm^{-1}h^{-1})$	$\Psi_{NL}(h^{-1})$	$\overline{E}(t)\ {}^{A}_{NL}\ x10^{-6}(m)$	β/γ	$R_A x10^{-6}(m)$
$(\mathfrak{L}_1)10.2$	0.0095	5.968	6.67567	5.40
$(\mathfrak{L}_2)51.2$	0.0077	18.952	2.64560	10.75
$(\mathfrak{L}_3)92.2$	0.0145	35.627	3.92871	13.10

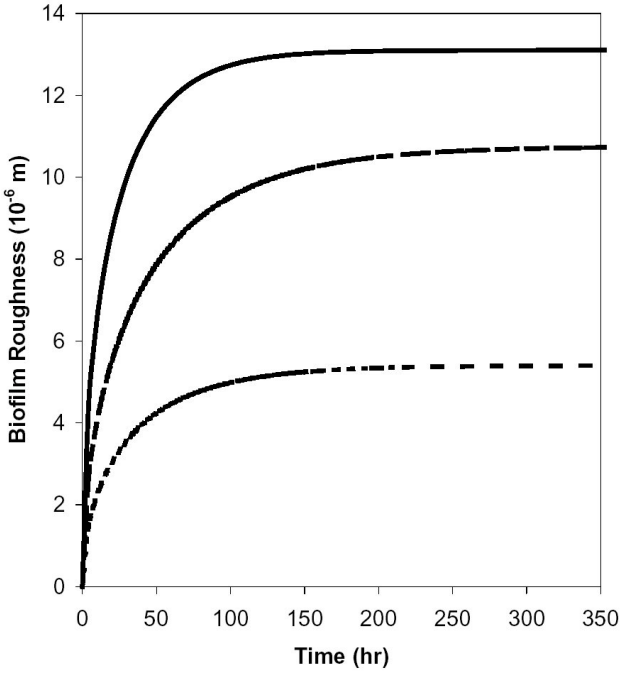

FIGURE 4. Biofilm roughness R_{NL} vs. t as calculated from Eq. (69) for the same P. Aeruginosa biofilm for the parameters given in Table IV. (- - -) $\mathfrak{L}_{01} = 10.2$, (— —) $\mathfrak{L}_{02} = 51.2$, (—) $\mathfrak{L}_{03} = 92.2$ $(mgm^{-1}h^{-1})$.

mental data, while the theoretical value by optimizing Ψ and $V\gamma$. It is important to point out that in this procedure only two parameters are optimized, namely, $\Psi/(V\gamma)$ and β/γ. Their optimal values turned out to be $\Psi = 0.3486$ and $V\gamma = 4.96x10^{-4}$. Note that the theoretical results show a nonlinear increase of $R(t)$ with $\left\langle \overline{E}(t) \right\rangle$ in correspondence with experimental observations [2, 6, 10]. However, it also shows a tendency to saturate to a constant value, in contrast to the numerical adjustment by Peyton. Therefore, we conclude that when the detachment of biomass exists, the nonlinear model exhibits the same basic behavior.

6. Concluding remarks

In summary, in this work we have presented and developed a stochastic approach to describe the thickness and roughness of a competitive growing population in a biofilm. To elaborate on the obtained results the following comments may be useful.

A stochastic model which describes in a unified form both, internal as well as external fluctuations in monospecies biofilms was proposed. It is important to stress that the model is idealized in many respects. To begin with, it assumes that all microorganisms have the same reproduction rate; it does not include the spatial heterogeneity of the biofilm and therefore, does not take into account the changes of the state variables due to substrate diffusion within the biofilm. For spatially inhomogeneous systems, fluctuations in the number of individuals are a local phenomenon and their description requires to know $n(\overrightarrow{r}, t)$. This can be accomplished by introducing the number density as a continuous random quantity, which amounts to describe the system in terms of an infinite set of stochastic variables. Although this continuous description may be achieved in a variety of ways [29, 30], its implementation is not an easy task and one has to restore to approximations, such as the method of compounding moments [15]. For this reason in this work we neglected spatial effects. The spatial distribution of adherent bacteria on the surface has been measured and taken into account in a description based on rate equations for the attached cells concentrations. This leads to the consideration of effective attachment rate constants dependent on position, because the number of cells near the surface that available for attachment may vary with the position [31]. In this way a spatial dependence in the transition probabilities per unit time could be introduced.

The age of the biofilm was neglected because the mechanisms that govern this phenomenon are not well known. However, this simplification is essential to use Markovian stochastic processes in modelling the elementary events. This was particularly useful since the theory of stochastic Markovian process is much more developed than its non-Markovian counterpart. On the other hand, the changes in the external conditions that necessarily influence the biofilm growth, were modeled through external noise in the rate of reproduction.

Biofilm roughness is only one of a series of problems in understanding biofilms. The internal structure of the biofilm (channels, pores, etc), state of the biomass (active, inactive, areas of extracellular material) and diffusive and convective flows through this structure are also of important significance. However, in spite of its limitations, this stochastic model is able to predict an explicit time dependence of average thickness and roughness, as well as a relationship between these two quantities, as discussed in section 4, while determinis-

tic models are not able to do so. Some of the limitations might be overcome in future works through stochastic generalizations that include spatial dependence and hydrodynamical effects. To this end Langevin descriptions or the use of the van Kampen's compounding moments method to include spatial dependence, could be explored. Also, the model can be extended to include multispecies biofilms by constructing a multivariate master equation; however, whether this generalizations are able to successfully model other features of biofilms, remains to be assessed.

Acknowledgment

One of us (RFR) would like to thank the warm hospitality and support of Area de Ingeniería de Recursos Energéticos, Dpto. I. P. H., UAM-I, where this work was done. He also acknowledges partial financial support from grants DGAPA-UNAM, IN101999.

The authors acknowledge Ms. E. Rodríguez for pointing out to us some relevant references.

∗. Fellow of SNI

1. J.W. Costerton, G.G. Geesey and K.J. Cheng, *Sci. Am.* **238** (1978) 86.
2. B. Peyton, *Wat. Res.* **30** (1996) 29.
3. P.A. Wilderer and W.G. Characklis, "Structure and Functions of Biofilms" in *Structure and Function of Biofilms*, W.G. Characklis and P.A. Wilderer, editors (Wiley, New York, 1989)
4. B. Rittmann, *Biotechnol. Bioeng.* **24** (1982) 1341.
5. W. Characklis, *Biotechnol. Bioeng.* **23** (1981) 1923.
6. P. Stewart, R. Murge, R. Srinivesan, and D. de Beer, *Wat. Res.* **29** (1995) 2006.
7. R. Murge, P. Stewart, and D. Daly, *Biotechnol. Bioeng.* **45** (1995) 503.
8. R. Srinivasan, P. Stewart, T. Griebe, Ch. Chen, and X. Xu, *Biotechnol. Bioeng.* **46** (1995) 553.
9. D. de Beer, P. Stoodley, F. Roe and Z. Lewandowski, *Biotechnol. Bioeng.* **43** (1994) 1131.
10. T. Zhang and P. Bishop, *Water Res.* **28** (1994) 2279.
11. D. de Beer, P. Stoodley and Z. Lewandowski, *Biotechnol. Bioeng.* **44** (1994) 636.
12. T. Zhang and P. Bishop, *Wat. Res.* **28** (1994) 2267.
13. B. Rittmann and J. Manem, *Biotechnol. Bioeng.* **39** (1992) 778.
14. B.F. Picologlou, N. Zelver and W.G. Characklis, *J. Hydraul. Division, Proc. ASCE* **106** (HY5) (1980) 733.
15. N.G. van Kampen, *Stochastic Processes in Physics and Chemistry* (Elsevier, Amsterdam,1992)
16. G.W. Gardiner, *Handbook of Stochastic Processes* (Springer Verlag, Berlin,1994)
17. S.S. Tambe, V. Ravikumar, B.D. Kulkarni and L.K. Doraiswamy, *Chem. Engn. Sci.* **40** (1985) 1951.
18. L.D. Landau and E.M. Lifshitz, *Statistical Physics* (Addison Wesley, Reading, 1970)
19. S.S. Tambe, B.D. Kulkarni and L.K. Doraiswamy, *Chem. Engn. Sci.* **40** (1985) 1943.
20. W. Horsthemke and R. Lefever, *Noise Induced Transitions*, Synergetics, Series, Vol. 15 (Springer Verlag, Berlin, 1983)
21. R.F. Rodríguez, E. Salinas-Rodríguez, A. Hayashi, A. Soria and J.M. Zamora, *AIChE J.* **47** (2001) 1721.
22. J.M. Sancho and M. San Miguel, *J. Stat. Phys.* **37** (1984) 151.
23. N.S. Goel and N. Richter-Dyn, *Stochastic Models in Biology* (Academic Press, New York, 1974)
24. W.G. Characklis, G. McFeters and K.C. Marshall, In Characklis, W.G., Marshall, K.C., editors *Biofilms* (New York, John Wiley & Sons, 1990) p. 341
25. W.G. Characklis, *Water Res.* **7** (1973) 1249.
26. E. Izquierdo Kulich, *Descripción Estocástica de Biopelículas en Filtros Percoladores*, Master in Chemical Engineering Thesis, National University of Mexico (in Spanish)(1998)
27. O. Wanner, A. Cunningham, and R. Lundman, *Biotechnol. Bioeng.* **47** (1995) 708.
28. H. Beyenal, Z. Lewandowski, *AIChE J.* **47** (2001) 1689.
29. S. Chaturvedi, C.W. Gardiner, I.S. Matheson and D.F. Walls, *J. Stat. Phys.* **17** (1977) 469.
30. C. van den Broeck, W. Horsthemke and M. Malek-Mansour, *Physica A* **89** (1977) 339.
31. R.B. Dickinson and S.L. Cooper, *AIChE J.* **41** (1995) 2160.